Report

Current Biology

Divergence and Functional Degradation of a Sex Chromosome-like Supergene

Graphical Abstract

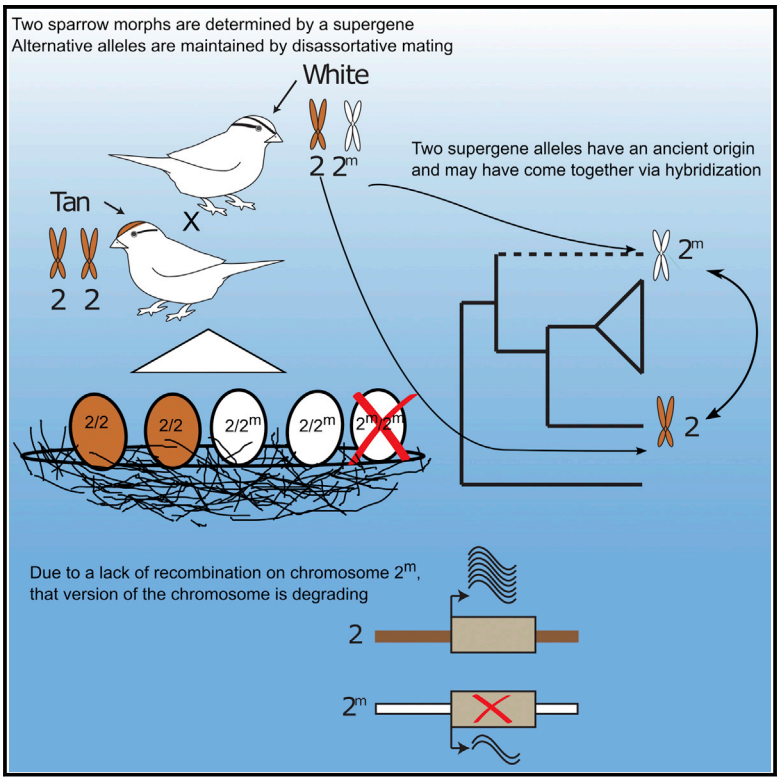

Highlights

- A balanced supergene determines disassortative mating between bird morphs
- One supergene allele appears to be degrading similar to neo-Y/W chromosomes
- Alternate alleles are ancient and likely became polymorphic via hybridization

Authors

Elaina M. Tuttle, Alan O. Bergland, Marisa L. Korody, ..., Wesley C. Warren, Rusty A. Gonser, Christopher N. Balakrishnan

Correspondence

elaina.tuttle@indstate.edu

In Brief

Supergenes are linked clusters of genes that contribute to adaptive variation. The origin and fate of polymorphic supergenes within species are not well understood. To advance the understanding of supergenes, Tuttle et al. examine the origin, evolutionary history, and possible fate of a fitness-related supergene in the white-throated sparrow.

Tuttle et al., 2016, Current Biology *26*, 1–7
February 8, 2016
http://dx.doi.org/10.1016/j.cub.2015.11.069

CellPress

Please cite this article in press as: Tuttle et al., Divergence and Functional Degradation of a Sex Chromosome-like Supergene, Current Biology (2016), http://dx.doi.org/10.1016/j.cub.2015.11.069

Current Biology
Report

Divergence and Functional Degradation of a Sex Chromosome-like Supergene

Elaina M. Tuttle,[1,6,*] Alan O. Bergland,[2,6] Marisa L. Korody,[1] Michael S. Brewer,[3] Daniel J. Newhouse,[3] Patrick Minx,[4] Maria Stager,[5] Adam Betuel,[1] Zachary A. Cheviron,[5] Wesley C. Warren,[4] Rusty A. Gonser,[1] and Christopher N. Balakrishnan[3]

[1]Department of Biology and The Center for Genomic Advocacy, Indiana State University, 600 Chestnut Street, Terre Haute, IN 47809, USA
[2]Department of Biology, Stanford University, 371 Serra Mall, Stanford, CA 94305-5020, USA
[3]Department of Biology, East Carolina University, Howell Science Complex, Greenville, NC 27858, USA
[4]McDonnell Genome Institute, Washington University School of Medicine, 4444 Forest Park Avenue, Campus Box 8501, St. Louis, MO 63108, USA
[5]Department of Animal Biology, School of Integrative Biology, University of Illinois, Urbana-Champaign, IL 61801, USA
[6]Co-first author
*Correspondence: elaina.tuttle@indstate.edu
http://dx.doi.org/10.1016/j.cub.2015.11.069

SUMMARY

A major challenge in biology is to understand the genetic basis of adaptation. One compelling idea is that groups of tightly linked genes (i.e., "supergenes" [1, 2]) facilitate adaptation in suites of traits that determine fitness. Despite their likely importance, little is known about how alternate supergene alleles arise and become differentiated, nor their ultimate fate within species. Herein we address these questions by investigating the evolutionary history of a supergene in white-throated sparrows, *Zonotrichia albicollis*. This species comprises two morphs, tan and white, that differ in pigmentation and components of social behavior [3–5]. Morph is determined by alternative alleles at a balanced >100-Mb inversion-based supergene, providing a unique system for studying gene-behavior relationships. Using over two decades of field data, we document near-perfect disassortative mating among morphs, as well as the fitness consequences of rare assortative mating. We use de novo whole-genome sequencing coupled with population- and phylogenomic data to show that alternate supergene alleles are highly divergent at over 1,000 genes and that these alleles originated prior to the split of *Z. albicollis* from its sister species and may be polymorphic in *Z. albicollis* due to a past hybridization event. We provide evidence that the "white" allele may be degrading, similar to neo-Y/W sex chromosomes. We further show that the "tan" allele has surprisingly low levels of genetic diversity yet does not show several canonical signatures of recurrent positive selection. We discuss these results in the context of the origin, molecular evolution, and possible fate of this remarkable polymorphism.

RESULTS AND DISCUSSION

Understanding how suites of adaptive characters remain linked despite the disruptive forces of recombination has been a major challenge in evolutionary biology. "Supergenes" are linked clusters of coevolved genes that, like sex chromosomes, give rise to divergent fitness-related traits that are variable within species [1, 2]. Nonetheless, how supergenes originate, generate adaptive variation, and are maintained and evolve within a species remain unclear. To examine these basic questions, we analyzed supergene evolution in the white-throated sparrow (*Zonotrichia albicollis*). The two plumage morphs (Figure 1A) of the white-throated sparrow differ dramatically in reproductive behavior [3, 5], representing two extremes in reproductive trade-offs: white males are promiscuous and invest heavily in securing additional matings at the expense of paternal care [3], whereas tan males are monogamous [3] and contribute more to parental care [6]; females exhibit similar trade-offs between investment in parental care versus mating effort [3].

Our long-term genotypic analysis builds on previous work [6, 7] and, through extensive genotyping of thousands of individuals over more than two decades, confirms that white morphs are almost always heterozygous for alternative chromosome *2* alleles ($2^m/2$). We find that 99.7% of white morphs are heterozygous (n = 1,014; Table S1), whereas tan morphs are always homozygous (*2*/*2*; 100%, n = 978). Thus, chromosomes *2* and 2^m segregate at ~75% and ~25% frequency, respectively, and the two plumage morphs occur in approximately equal numbers. Chromosome *2* remains polymorphic via near-obligate mating between tan and white morphs (i.e., disassortative mating) [8]. Only 17 out of 1,116 pairs (1.5%) observed in this study mated with an individual of the same morph (i.e., homotypic or assortative mating). Homotypic pairs are even less common in primary pairings (9/1,106, 0.8%), but occur more commonly in secondary pairings (8/10, 80%; Table S2) following the disappearance of an opposite-morph mate and when mate-choice options are limited. As a consequence of obligate disassortative mating the species effectively has four sexes, wherein any individual can mate with only 1/4 of the individuals in the population.

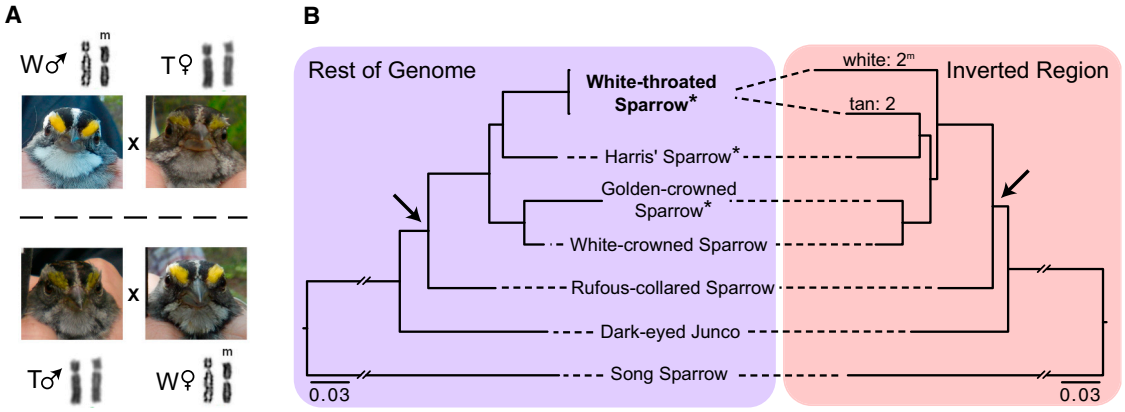

Figure 1. White-Throated Sparrows Comprise Two Morphs with an Ancient Origin

(A) Tan (T) and white (W) morph sparrows (note differences in plumage color in the head stripe and throat) differ in chromosome *2* (sometimes referred to as ZAL2) genotype and mate almost exclusively with the opposite morph, maintaining polymorphism in the species.

(B) Tan (*2*) and white (2^m) chromosomes are highly divergent within the inverted portion of the chromosome, suggesting an ancient origin of the chromosomes *2* and 2^m. All nodes are supported by 100% bootstrap values, and the depicted topology for the inverted region is a significantly better fit to the data than trees constrained to the monophyly of *2* and 2^m ($p < 0.001$; see the Supplemental Experimental Procedures). Taxa marked with an asterisk are those for which whole genomes were sequenced. The arrows highlight the ancestral node for the Zonotrichia genus.

See also Table S2.

Given the myriad phenotypic and behavioral differences controlled by this inversion polymorphism [3] and the unusual dynamics of the mating system, the white-throated sparrow harbors a classic example of a balanced supergene [9]. To resolve the evolutionary history of this supergene, we first sequenced and assembled the genome of a single tan male (homozygous *2/2* and *Z/Z*; Figure 1), resulting in a draft genome 1.03 Gb long, comprising 6,018 scaffolds, 13,811 protein-coding genes, 1,104 non-coding transcripts, and 205 pseudogenes. The assembled genome has a contig N50 of 113 kb and a scaffold N50 of 4.9 Mb, comparable or better than most recent short-read-based bird assemblies [10].

Pooled whole-genome resequencing of 24 tan and 25 white males revealed a bimodal distribution of scaffold-wide average F_{ST} between morphs estimated from 18.4 million biallelic SNPs and polymorphic indels (collectively, "variants"; Figure S1). Previous studies [11] revealed high differentiation between *2* and 2^m, and we reasoned that high F_{ST} scaffolds would correspond to regions within the chromosome *2* inversion. We confirmed this by associating a subset of assembled scaffolds with fluorescence in situ hybridization (FISH)-mapped bacterial artificial chromosomes (BACs). Scaffolds associated with BACs known to map within the inversion had correspondingly high F_{ST} (median 0.3; Table S3). The scaffolds that map to the region near the distal end of the inverted region on *2* have decreased average F_{ST} (~0.2; Figure 2A; Table S3) and a significantly higher rate of shared polymorphism between *2* and 2^m (odds ratio 5.73, Fisher's exact test, $p < 1e\text{-}10$), suggesting that limited recombination or gene conversion occurs between *2* and 2^m in this region. However, the extent of genetic exchange in this region or the rest of the inversion is presently unknown. High F_{ST} (≥ 0.2) scaffolds include 1,137 genes that comprise the supergene. F_{ST} is expected to be 0.33 at variants that are fixed between *2* and 2^m in comparisons between tan (*2/2*) and white ($2/2^m$) birds. Approximately 78.6% of the 1.5-Mb variants (or ~1/100 bp) within the inversion have an F_{ST} of ~0.33 (Figure S1B), demonstrating that the majority of variants in the inversion are heterozygous among all the white birds we sampled. To confirm fixed differences between 2^m and *2* identified in pooled genotypes, we resequenced the genomes of three individual white-morph birds sampled from a different population from the pooled sample. We find that 75% of variants within the inversion are heterozygous in all three birds; note that, given limited sequencing depth of individual birds (~10×), we expect a fraction of truly polymorphic variants to appear homozygous, thus explaining the discrepancy between the rate of fixed differences (75% versus 78.6%, respectively) observed in our individual and pooled-based resequencing. In addition, we estimated linkage disequilibrium (r^2) within the pooled samples. As expected, r^2 is ~1 within the inverted region among the pool of white birds (Figure 2C).

The inversion contains a number of well-studied genes related to the neurophysiological control of behavior, including multiple steroid hormone receptors (Table 1). ESR1 has already been implicated as contributing to behavioral differences between white-throated sparrow morphs [12], and VIP has been shown to mediate variation in aggressive behavior in other songbirds [13, 14]. Within this gene complex are also two genes with annotated roles in pigmentation (FIG4 and LYST [15]). We note, however, that none of these genes show extreme signatures of recent positive selection (see below) or unusual patterns of divergence relative to other genes within the inversion. Indeed, the high levels of divergence throughout the inversion provide a challenge in resolving the relative contributions of specific genes to the suite of phenotypic differences among morphs.

The high level of nucleotide divergence between chromosomes *2* and 2^m suggests that the divergence of these chromosomes predates the divergence of the white-throated sparrow and its sister species. To investigate the long-term

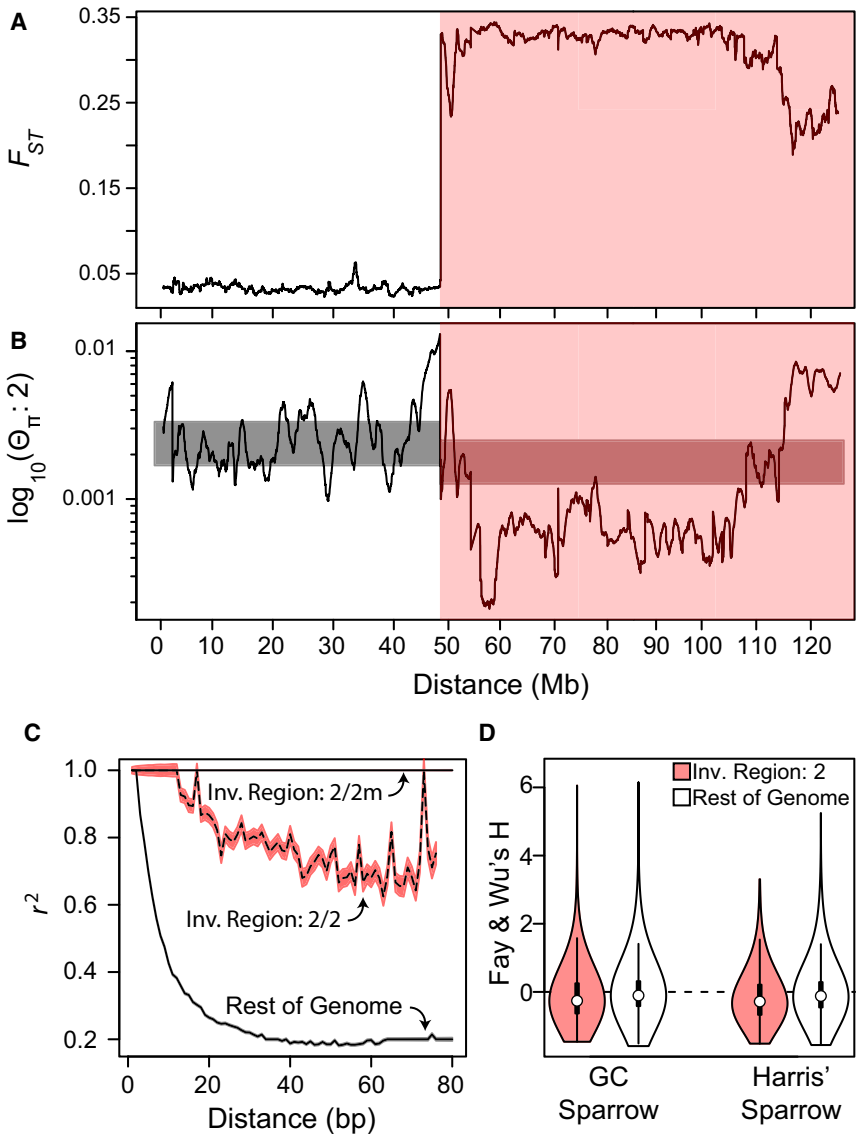

Figure 2. Contrasting Divergence, Diversity, and Linkage Disequilibrium

(A and B) Sliding window estimate across FISH-mapped scaffolds of (A) F_{ST} between white and tan birds and (B) genetic diversity along the tan allele, *2*. The gray bars represent the 95% confidence band (SD). The pink area indicates the region inside the inversion, whereas the uncolored area represents the area outside the inversion.

(C) Linkage disequilibrium decays rapidly outside of the inversion, but is high, especially in $2/2^m$ heterozygotes, within the inversion.

(D) Using golden-crowned (GC) or Harris's sparrows as outgroups, Fay and Wu's H estimates [26] do not show a strong signal of recent selective sweeps in the inverted region of chromosome *2*.

See also Figures S1 and S3 and Table S3.

evolutionary history of chromosomes *2* and 2^m, we examined genome-wide patterns of divergence between the white-throated sparrow and its close relatives. For comparison, we analyzed closely related taxa with previously [16, 17] or newly sequenced transcriptomes or genomes (Figure 1B). As in previous studies [11], we find that the relationship of chromosomes *2* and 2^m conflicts with the species tree and suggests more recent common ancestry of chromosome *2* with other taxa than with 2^m. Our genome-scale analyses and complete taxon sampling of the Zonotrichia genus revealed that outside the inversion, the white-throated sparrow is sister to Harris's sparrow. This same relationship holds for the tan (*2*) allele within the inversion. Inclusion of the rufous-collared sparrow in our analysis allowed us to resolve that the white 2^m allele arose after the origin of Zonotrichia and falls sister to the rest of the clade.

Because 2^m exists almost exclusively in a non-recombining heterozygous state (Table S1), it has been hypothesized that 2^m may be degrading in a manner that is similar to neo-Y/W chromosomes [18, 19]. Huynh and colleagues [19], using a smaller set of markers, failed to find an enrichment of non-synonymous changes on 2^m, and thus concluded that the chromosome was not degrading. In contrast, here we provide evidence consistent with functional degradation of 2^m by first using genome-wide estimates of polymorphism and divergence at non-synonymous and synonymous sites (Figure 3A). We calculated the direction of selection (DoS) statistic [20], which is conceptually related to the McDonald-Kreitman test, to compare the relative rates of non-synonymous and synonymous polymorphism to non-synonymous and synonymous divergence. On average, genes inside the inverted region that are linked to 2^m have a significantly negative DoS ($p_{golden\text{-}crowned} < 0.001$; $p_{Harris's} < 0.001$), indicating an excess of non-synonymous polymorphism and consistent with functional degradation of 2^m. Outside the inversion, the DoS is slightly positive, indicating a small excess of non-synonymous fixed differences between the white-throated sparrow and either of two outgroup species ($p_{golden\text{-}crowned} = 0.059$; $p_{Harris's} < 0.001$). Genes inside the inverted region that are linked to *2* do not show a significant deviation from expectation based on a randomization test ($p > 0.05$ for both outgroups). Intriguingly, fixed differences between *2* and 2^m are only slightly more likely to be non-synonymous relative to expectations from interspecific divergence [$p_{golden\text{-}crowned} < 0.001$; $p_{Harris's} < 0.001$; see Figure 3A, Inv. (2/2m)]. This latter result suggests that chromosome *2* has relatively recently become polymorphic in the white-throated sparrow: long-term heterozygosity of 2^m would most likely lead to fixation of putatively deleterious non-synonymous mutations, giving rise to a DoS between *2* and 2^m (Figure 3) that is similar

Table 1. Candidate Genes for Behavior and Pigmentation

Gene	Gene Name	Exon (NS/S)	Intron	UTR (5′/3′)	Up	Down
CGA	glycoprotein hormones, alpha polypeptide	0/1	34	0/4	51	71
ESR1	estrogen receptor 1	2/4	2,565	0/14	53	54
ESRRG	estrogen related receptor gamma	1/3	2,465	0/17	52	68
FSHR	follicle stimulating hormone receptor	6/11	1,291	0/8	112	5
HTR1B	Serotonin receptor 1B	0/4	1	7/3	46	59
HTR1E	Serotonin receptor 1E	2/7	0	1/4	78	65
LHCGR	luteinizing hormone/ choriogonadotropin receptor	5/14	285	0/0	103	44
VIP	vasoactive intestinal peptide	0/0	79	4/1	99	104
FIG4	FIG4 homolog	3/11	470	3/5	154	67
LYST	lysosomal trafficking regulator	19/48	931	2/19	56	0

Fixed differences between chromosomes *2* and 2^m in candidate genes for behavior and pigmentation (FIG4 and LYST). Polymorphisms are divided by site class including exons (non-synonymous [NS]/synonymous [S] substitutions), introns, UTR (5′/3′), and 1 kb up- and downstream of start and stop codons, respectively.

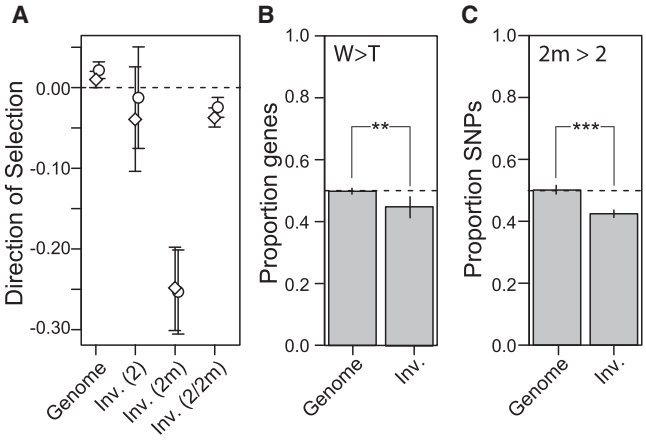

Figure 3. Functional Degradation of 2^m

(A) Using two different outgroups (diamond, golden-crowned sparrow; circle, Harris' sparrow), the direction of selection statistic is strongly negative on 2^m, indicating an increased level of non-synonymous polymorphism. When the DoS is calculated between *2* and 2^m (Inv. 2/2m), the signature is similar to the neutral expectation, suggesting that the two alleles came together only recently.

(B) For genes within the inversion, gene expression is higher for tan birds than heterozygous ($2/2^m$) white-morph birds.

(C) In white birds, the white (2^m) allele tends to be underexpressed relative to the tan (*2*) allele.

**p < 0.01; ***p < 0.001. Error bars represent 95% confidence intervals (SE). See also Figures S2 and S4 and Table S1.

in magnitude to the DoS statistic based on polymorphisms segregating on 2^m.

In neo-sex chromosomes, functional degradation is accompanied by decreased average gene expression of Y/W-linked genes [21, 22]. We contrasted gene expression levels between three tan and three white birds and also measured patterns of allele-specific expression within white birds. On average, the expression level of genes within the inverted region is lower in white birds than tan birds (Figure 3B), and expression of the allele linked to 2^m is lower than the allele linked to *2* within heterozygous white birds (Figure 3C). Differences in gene expression between *2*- and 2^m-linked genes are subtle (Figure S2), and may reflect tissue-specific effects or a relatively recent degradation of 2^m. Decreased expression of 2^m-linked genes is not an artifact of increased general expression of *2*-linked genes, as seen by a comparison of log-transformed expression levels of genes inside the inverted region versus the rest of the genome within tan birds ($t = 0.0324$, $p = 0.97$). Whereas differences in expression levels of some genes inside the inverted region likely contribute to adaptive differentiation between morphs, our results suggest that 2^m is degrading.

As in sex chromosomes, we hypothesized that pairwise genetic diversity (Θ_π) on *2* and 2^m would be 75% and 25% of that in the rest of the genome, respectively [23]. In contrast, Θ_π on *2* is only ~30% of background diversity (0.0007 versus 0.0023; Figure 2B) and Θ_π on 2^m is only ~20% of background (0.00047 versus 0.0023; Figure S3), indicating that diversity on these chromosomes is not at the expected equilibrium under a simple neutral model. In sex chromosomes, departures from equilibrium diversity ratios have been attributed to multiple forces, including differences in life history between sexes [24] and differences in how natural selection and genetic drift operate. One component of life history that could influence patterns of diversity is differences in the variance of reproductive success between morphs. In white-throated sparrows, if tan birds have a higher variance in reproductive success the ratio of diversity between *2* and the genomic background will be >75%, whereas if white birds have a higher variance in reproductive success the ratio will be <75% [24]. To assess whether the observed deviations from expected patterns of genetic diversity could be attributed to life-history variation among morphs, we calculated lifetime reproductive success among 255 white and tan adult birds. We find no significant difference in the variance of reproductive success among morphs (Levene test, $p = 0.84$). Thus, life-history variation among morphs may play a limited role in shaping patterns of genetic variation between inverted and non-inverted regions of the genome; however, we cannot reject more complicated demographic scenarios at the present time [25].

The differential action of natural selection is another factor that can influence the ratio of genetic diversity between the X/Z chromosomes and autosomes and, by extension, chromosomes *2* and 2^m. On the white allele, 2^m, which is analogous to Y/W chromosomes, the lack of recombination makes discerning signatures of selection challenging, so we focused analyses of selection on the tan allele, *2*. On *2*, like X/Z chromosomes, beneficial mutations may be more likely to go to fixation (positive selection) and deleterious mutations may be more likely to be purged (purifying selection) because of functional hemizygosity in white $2/2^m$ birds [24]. Either positive or negative selection would lead to a decrease in genetic diversity on *2*, and could possibly explain the substantial reduction of diversity and

elevated linkage disequilibrium observed on this chromosome (Figure 2B). Under a scenario of widespread positive selection along the inverted region of *2*, we would expect a substantial increase in the proportion of high-frequency derived alleles that would be revealed by negative values of Fay and Wu's H [26]. We calculated Fay and Wu's H using either Harris's or golden-crowned sparrows as outgroups. H is slightly more negative inside the inverted region of *2* than outside, but does not show an excess of extremely negative H values (Figure 2D). Widespread positive selection along the inverted region of *2* may also lead to a slight excess of fixed non-synonymous differences; however, no such pattern is observed (Figure 3A). Although positive selection has likely shaped patterns of genetic variation at certain loci of the inverted region of *2*, current tests fail to resolve systematic evidence for increased rates of positive selection on *2*. The reduction in diversity along *2* relative to the genomic background could therefore be influenced by strengthened purifying selection arising as a consequence of functional degradation of chromosome 2^m, strengthened background selection arising as a consequence of reduced recombination rate, as well as occasional selective sweeps at specific loci.

Given the strength of disassortative mating and evidence for degradation of chromosome 2^m, we hypothesized that there are fitness consequences associated with homotypic mating. White male × white female (WxW) homotypic pairs are expected to produce, on average, 25% "superwhite" $2^m/2^m$ homozygotes, potentially exposing deleterious recessive alleles that have arisen on 2^m. In 27 years of study, we have found only 3 superwhite $2^m/2^m$ birds out of 1,989 (0.15%) genotyped birds. Based on the observed frequency of mating between white-morph males and females, both via social pairing and extrapair mating, we expected 12 superwhites in our sample (see the Supplemental Experimental Procedures). The lower than expected number of observed superwhites (Fisher's exact test, $p = 0.035$) suggests that the $2^m/2^m$ genotype is deleterious (Table S1), parents reduce investment in such offspring [27], or both. Whereas the two observed female superwhites appeared normal in size, the one superwhite male we found was over 2.5 SDs smaller than all other age-matched chicks and is the smallest male nestling sampled to date (Figure S4), suggesting that $2^m/2^m$ might be more deleterious in males. Occasional recombination on 2^m when superwhites do survive and reproduce may also mitigate the degradation of this chromosome.

Homotypic pairings of both types (WxW and TxT) suffer additional fitness costs. For example, different pairings (WxW, TxT, TxW, and WxT) suffer different rates of extrapair paternity in their nests ($F_{3,380} = 20.10$, $p < 0.0001$; Table S4). Like white male × tan female (WxT) pairs, both WxW and TxT pairs experience a significant (~25%) increase in extrapair paternity in their nests relative to tan male × white female (TxW) pairs (Tukey-Kramer post hoc tests, $p < 0.05$). We also find that homotypic pairs show a tendency toward producing female-biased clutches (homotypic pairs [n = 12], 37% ± 9% males; heterotypic pairs [n = 284], 52% ± 1% males; $F_{1,294} = 2.66$, $p = 0.10$; Table S4). Because many species adaptively adjust offspring sex ratios to produce a higher proportion of offspring of the smaller sex (females, in the case of the white-throated sparrow) when they are in poor condition or under stress [28], such data suggest that homotypic pairs are at a disadvantage. Last, although chicks raised by TxT pairs are similar in mass to disassortative pairs, chicks raised by WxW pairs are significantly smaller than those raised by TxT pairs ($F_{1,30} = 11.57$, $p = 0.0019$), likely a result of reduced parental care by white-morph birds. This pattern is primarily driven by mass differences in male chicks, because sons from WxW pairs are significantly smaller than sons from TxT pairs ($F_{1,12} = 7.45$, $p = 0.01$), whereas the mass of daughters does not differ by pair type ($F_{1,16} = 2.85$, $p = 0.11$). These costs associated with homotypic pairing may contribute to the maintenance of the chromosomal polymorphism in the species by favoring disassortative pairing.

Two plausible models explain the presence of both *2* and 2^m in white-throated sparrows subsequent to their ancient divergence: either these chromosomes were polymorphic in an ancestral Zonotrichia species but remain so only in white-throated sparrows, or one of the chromosomes entered the white-throated sparrow via hybridization followed by adaptive introgression (Figure 1B). Previous studies favored the former scenario [11], because no potential hybridizing taxon was found [11]. As we discuss above, however, patterns of polymorphism on chromosome 2^m (Figure 3A) suggest that this chromosome may have become polymorphic in the white-throated sparrow relatively recently. Although the lack of a clear sister species to 2^m is challenging for this interpretation, complete genus-level taxon sampling suggests that the donor species of 2^m may be extinct. In support of the model that 2^m is polymorphic in the white-throated sparrow via introgression, we note that hybridization between various Zonotrichia species has been observed in the wild [29] and inferred from discordance between mitochondrial and nuclear phylogenies [30]. Origination of supergene alleles in separate species provides a simple mechanism by which coadapted gene complexes can be formed, and under which recombination suppression between alleles would be expected when heterokaryotypes arise via hybridization [9].

Chromosomes *2* and 2^m in white-throated sparrows are independent of sex chromosomes but show striking parallels with patterns of sex chromosome divergence and degradation [31, 32]. Indeed, because of disassortative mating based on both chromosomes *2* and 2^m and the W and Z sex chromosomes, the species operates as though there are four sexes. Sexual systems with more than two sexes are exceedingly rare among animals, and theory predicts that they are unlikely to persist for long periods of time [33]. In part, this instability arises because four-sex systems have a 2-fold increase in some aspects of reproductive effort, such as finding a mate. If such four-sex systems are truly unstable, the persistence of the inversion-based plumage morph polymorphism found in the white-throated sparrow may be transient, despite the observed fitness benefits of disassortative mating.

ACCESSION NUMBERS

The accession number for the *Z. albicollis* whole-genome assembly reported in this paper is GenBank: GCA_000385455.1. The accession number for the *Zonotrichia capensis* RNA-seq data reported in this paper is GenBank: PRJNA298255. The accession numbers for the pooled resequencing data for *Z. albicollis* reported in this paper are GenBank: SRR2012823 and SRR2012824. Finally, the accession numbers for individual resequencing data are GenBank: SRS930390, SRS930391, and SRS930394 for

Z. albicollis, GenBank: SRS1162844 for *Zonotrichia querula*, and GenBank: SRS1162859 for *Zonotrichia atricapilla*.

SUPPLEMENTAL INFORMATION

Supplemental Information includes Supplemental Experimental Procedures, four figures, and four tables and can be found with this article online at http://dx.doi.org/10.1016/j.cub.2015.11.069.

AUTHOR CONTRIBUTIONS

E.M.T. provided project leadership, designed the project, and prepared the manuscript; A.O.B. designed the project, performed analysis, and prepared the manuscript; M.L.K. performed FISH analysis; M.S.B. performed phylogenetic analysis of transcriptome data; D.J.N. performed analysis of pooled sequencing data; P.M. performed genome assembly and curation; M.S. performed RNA sequencing of *Junco hyemalis* and prepared the manuscript; A.B. analyzed field data; Z.A.C. performed RNA sequencing of *Z. capensis* and prepared the manuscript; W.C.W. provided project leadership, prepared the manuscript, and performed genome sequencing; R.A.G. designed the project and collected field data; and C.N.B. provided project leadership, designed the project, performed analysis, and prepared the manuscript.

ACKNOWLEDGMENTS

Funding for this work was provided by NIH NIGMS grant 1R01GM084229 (E.M.T. and R.A.G.), Indiana State University (E.M.T. and R.A.G.), and East Carolina University (C.N.B.). A.O.B. was supported by an NIH National Research Service Award (F32 GM097837) and by NIH grant R01GM100366 to Dmitri Petrov and Paul Schmidt. All experimental procedures involving live animals were approved by the Indiana State University Institutional Animal Care and Use Committee (protocols 562158-1:ET/RG and 562192-1:ET/RG). We thank the production sequencing group of the McDonnell Genome Institute at Washington University for library construction, sequencing, and data curation for the white-throated sparrow genome. The University of Alaska Museum kindly provided the *Z. atricapilla* and *Z. querula* samples. Dr. Alvaro Hernandez and the High-Throughput Sequencing and Genotyping Unit at the University of Illinois performed library preparation and genome resequencing. Marlys Houck and Oliver Ryder at the Institute for Conservation Research at the San Diego Zoo provided assistance with cell culture and karyotyping, and Michael Romanov helped with BAC identification. We thank Teri Lear and Judy Lundquist from the Gluck Equine Research Center at the University of Kentucky for fluorescence in situ hybridization. Finally, we thank the 1988–2014 white-throated sparrow field and laboratory research crews.

Received: June 18, 2015
Revised: October 12, 2015
Accepted: November 25, 2015
Published: January 21, 2016

REFERENCES

1. Kunte, K., Zhang, W., Tenger-Trolander, A., Palmer, D.H., Martin, A., Reed, R.D., Mullen, S.P., and Kronforst, M.R. (2014). doublesex is a mimicry supergene. Nature *507*, 229–232.
2. Wang, J., Wurm, Y., Nipitwattanaphon, M., Riba-Grognuz, O., Huang, Y.-C., Shoemaker, D., and Keller, L. (2013). A Y-like social chromosome causes alternative colony organization in fire ants. Nature *493*, 664–668.
3. Tuttle, E.M. (2003). Alternative reproductive strategies in the white-throated sparrow: behavioral and genetic evidence. Behav. Ecol. *14*, 425–432.
4. Formica, V.A., and Tuttle, E.M. (2009). Examining the social landscapes of alternative reproductive strategies. J. Evol. Biol. *22*, 2395–2408.
5. Knapton, R.W., and Falls, J.B. (1983). Differences in parental contribution among pair types in the polymorphic white-throated sparrow. Can. J. Zool. *61*, 1288–1292.
6. Thorneycroft, H.B. (1966). Chromosomal polymorphism in the white-throated sparrow, *Zonotrichia albicollis* (Gmelin). Science *154*, 1571–1572.
7. Thorneycroft, H.B. (1975). A cytogenetic study of white-throated sparrow, *Zonotrichia albicollis* (Gmelin). Evolution *29*, 611–621.
8. Lowther, J.K. (1961). Polymorphism in the white-throated sparrow *Zonotrichia albicollis* (Gmelin). Can. J. Zool. *39*, 281–292.
9. Schwander, T., Libbrecht, R., and Keller, L. (2014). Supergenes and complex phenotypes. Curr. Biol. *24*, R288–R294.
10. Frankl-Vilches, C., Kuhl, H., Werber, M., Klages, S., Kerick, M., Bakker, A., de Oliveira, E.H.C., Reusch, C., Capuano, F., Vowinckel, J., et al. (2015). Using the canary genome to decipher the evolution of hormone-sensitive gene regulation in seasonal singing birds. Genome Biol. *16*, 19.
11. Thomas, J.W., Cáceres, M., Lowman, J.J., Morehouse, C.B., Short, M.E., Baldwin, E.L., Maney, D.L., and Martin, C.L. (2008). The chromosomal polymorphism linked to variation in social behavior in the white-throated sparrow (*Zonotrichia albicollis*) is a complex rearrangement and suppressor of recombination. Genetics *179*, 1455–1468.
12. Horton, B.M., Hudson, W.H., Ortlund, E.A., Shirk, S., Thomas, J.W., Young, E.R., Zinzow-Kramer, W.M., and Maney, D.L. (2014). Estrogen receptor α polymorphism in a species with alternative behavioral phenotypes. Proc. Natl. Acad. Sci. USA *111*, 1443–1448.
13. Goodson, J.L. (1998). Territorial aggression and dawn song are modulated by septal vasotocin and vasoactive intestinal polypeptide in male field sparrows (*Spizella pusilla*). Horm. Behav. *34*, 67–77.
14. Goodson, J.L., and Adkins-Regan, E. (1999). Effect of intraseptal vasotocin and vasoactive intestinal polypeptide infusions on courtship song and aggression in the male zebra finch (*Taeniopygia guttata*). J. Neuroendocrinol. *11*, 19–25.
15. Ashburner, M., Ball, C.A., Blake, J.A., Botstein, D., Butler, H., Cherry, J.M., Davis, A.P., Dolinski, K., Dwight, S.S., Eppig, J.T., et al. (2000). Gene ontology: tool for the unification of biology. Nat. Genet. *25*, 25–29.
16. Balakrishnan, C.N., Mukai, M., Gonser, R.A., Wingfield, J.C., London, S.E., Tuttle, E.M., and Clayton, D.F. (2014). Brain transcriptome sequencing and assembly of three songbird model systems for the study of social behavior. PeerJ *2*, e396.
17. Stager, M., Swanson, D.L., and Cheviron, Z.A. (2015). Regulatory mechanisms of metabolic flexibility in the dark-eyed junco (*Junco hyemalis*). J. Exp. Biol. *218*, 767–777.
18. Davis, J.K., Mittel, L.B., Lowman, J.J., Thomas, P.J., Maney, D.L., Martin, C.L., and Thomas, J.W.; NISC Comparative Sequencing Program (2011). Haplotype-based genomic sequencing of a chromosomal polymorphism in the white-throated sparrow (*Zonotrichia albicollis*). J. Hered. *102*, 380–390.
19. Huynh, L.Y., Maney, D.L., and Thomas, J.W. (2011). Chromosome-wide linkage disequilibrium caused by an inversion polymorphism in the white-throated sparrow (*Zonotrichia albicollis*). Heredity (Edinb) *106*, 537–546.
20. Stoletzki, N., and Eyre-Walker, A. (2011). Estimation of the neutrality index. Mol. Biol. Evol. *28*, 63–70.
21. Bachtrog, D. (2006). Expression profile of a degenerating neo-Y chromosome in *Drosophila*. Curr. Biol. *16*, 1694–1699.
22. Hough, J., Hollister, J.D., Wang, W., Barrett, S.C.H., and Wright, S.I. (2014). Genetic degeneration of old and young Y chromosomes in the flowering plant *Rumex hastatulus*. Proc. Natl. Acad. Sci. USA *111*, 7713–7718.
23. Charlesworth, B. (2001). The effect of life-history and mode of inheritance on neutral genetic variability. Genet. Res. *77*, 153–166.
24. Charlesworth, B., Coyne, J.A., and Barton, N.H. (1987). The relative rates of evolution of sex chromosomes and autosomes. Am. Nat. *130*, 113–146.
25. Ramachandran, S., Rosenberg, N.A., Feldman, M.W., and Wakeley, J. (2008). Population differentiation and migration: coalescence times in a two-sex island model for autosomal and X-linked loci. Theor. Popul. Biol. *74*, 291–301.

26. Fay, J.C., and Wu, C.I. (2000). Hitchhiking under positive Darwinian selection. Genetics *155*, 1405–1413.

27. Pryke, S.R., and Griffith, S.C. (2009). Genetic incompatibility drives sex allocation and maternal investment in a polymorphic finch. Science *323*, 1605–1607.

28. Bonier, F., Martin, P.R., and Wingfield, J.C. (2007). Maternal corticosteroids influence primary offspring sex ratio in a free-ranging passerine bird. Behav. Ecol. *18*, 1045–1050.

29. Payne, R.B. (1979). Two apparent hybrid *Zonotrichia* sparrows. Auk *96*, 595–599.

30. Weckstein, J.D., Zink, R.M., Blackwell-Rago, R.C., and Nelson, D.A. (2001). Anomalous variation in mitochondrial genomes of white-crowned (*Zonotrichia leucophrys*) and golden-crowned (*Z. atricapilla*) sparrows: pseudogenes, hybridization, or incomplete lineage sorting? Auk *118*, 231–236.

31. Bellott, D.W., Hughes, J.F., Skaletsky, H., Brown, L.G., Pyntikova, T., Cho, T.-J., Koutseva, N., Zaghlul, S., Graves, T., Rock, S., et al. (2014). Mammalian Y chromosomes retain widely expressed dosage-sensitive regulators. Nature *508*, 494–499.

32. Cortez, D., Marin, R., Toledo-Flores, D., Froidevaux, L., Liechti, A., Waters, P.D., Grützner, F., and Kaessmann, H. (2014). Origins and functional evolution of Y chromosomes across mammals. Nature *508*, 488–493.

33. Hurst, L.D. (1996). Why are there only two sexes? Proc. R. Soc. Lond. B Biol. Sci. *263*, 415–422.

Current Biology

Supplemental Information

Divergence and Functional Degradation of a Sex Chromosome-like Supergene

Elaina M. Tuttle, Alan O. Bergland, Marisa L. Korody, Michael S. Brewer, Daniel J. Newhouse, Patrick Minx, Maria Stager, Adam Betuel, Zachary A. Cheviron, Wesley C. Warren, Rusty A. Gonser, and Christopher N. Balakrishnan

SUPPLEMENTAL INFORMATION

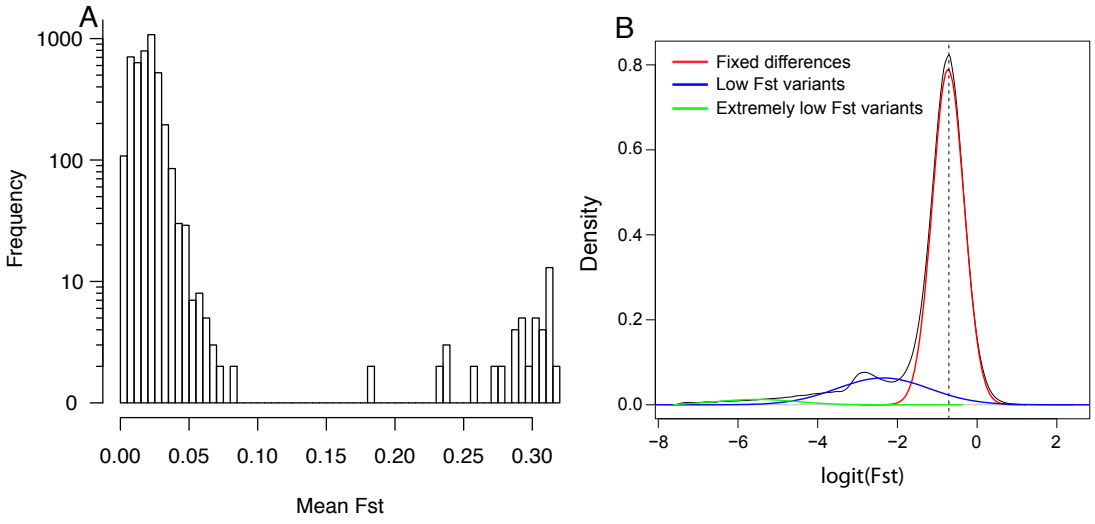

Figure S1, related to Figure 2 . A) Distribution of scaffold wide average F_{ST} among the ~6,000 assembled scaffolds. B) Distribution of variant F_{ST} values between white and tan birds within the *2 - 2^m* inversion. The distribution of F_{ST} is trimodal (χ^2 = 158, *df* = 3, p < 1e-50), with the largest component (red line; ~78.5% of variants) representing variants with F_{ST} ~ 0.33 (dashed vertical line). Other modes represent low F_{ST} variants (blue line, ~18.5% of variants), that are composed of polymorphisms segregating at low frequencies among either the white or tan birds, or extremely low frequency variants (green line, ~3% of variants) largely representing shared polymorphisms between white and tan birds.

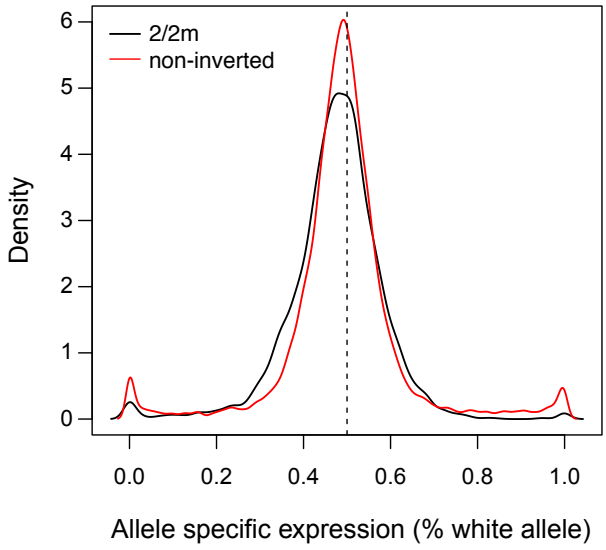

Figure S2, related to Figure 3. Distribution of allele specific expression values among three heterozygous white birds for variants inside (red line) and outside the *2/2^m* inversion. Dotted vertical line shows the expected allele specific expression value of 50%. In general, expression of *2^m*-linked genes is only mildly reduced relative to their *2*-linked homologues perhaps as a consequence of purifying selection acting to maintain proper dosage and the mitigating effects of double-recombination events or gene-conversion between *2* and *2^m*.

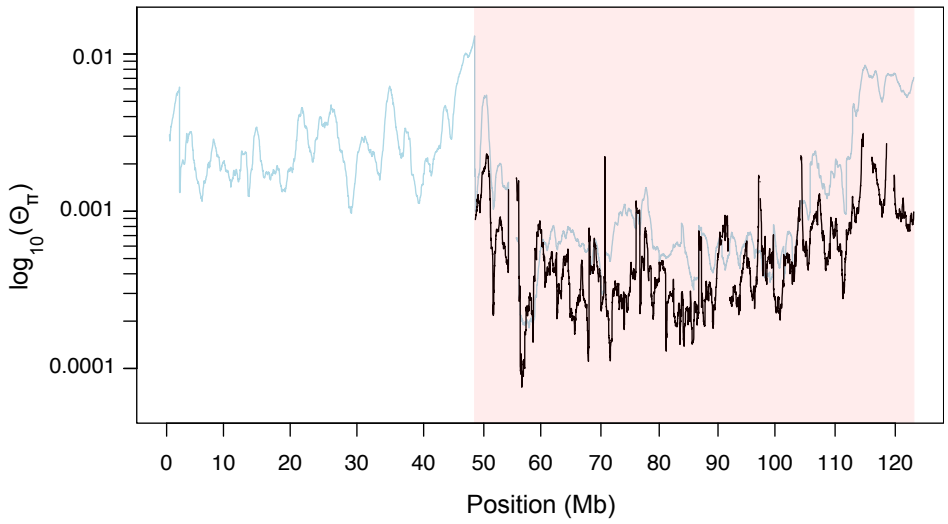

Figure S3, related to Figure 2. Sliding window estimates of diversity along chromosome 2^m (black line). For contrast, sliding window estimates of diversity along chromosome *2* are redrawn from Figure 2B (light blue).

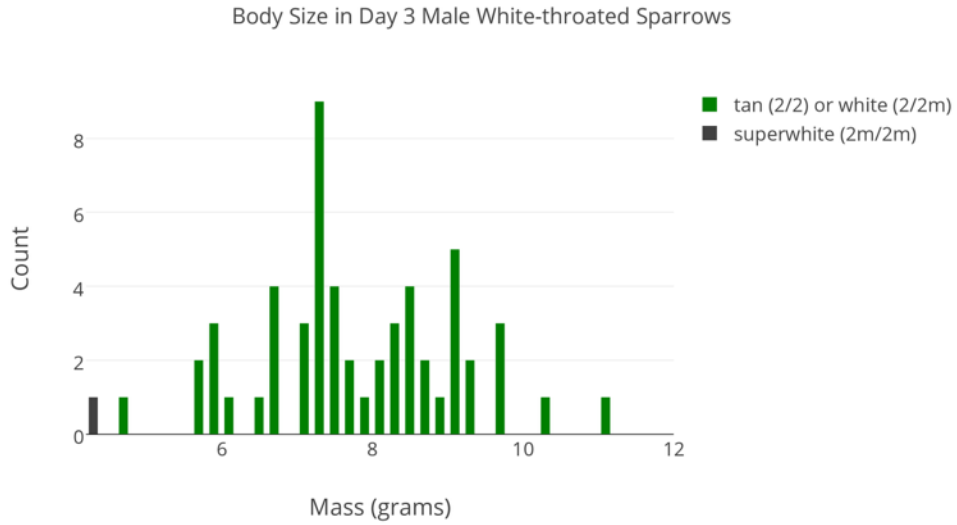

Figure S4, related to Figure 3. Body mass in 3 day old male chicks. One superwhite ($2^m/2^m$) male is the smallest male measured to date.

Morph	Tan (2/2)		White (2/2m)		Superwhite (2m/2m)		Total
Sex	male	female	male	female	male	female	
This Study	492	486	536	475	1*	2	1989
Thorneycroft[S1]	-	-	-	-	0	1	397
Michopoulus et al[S1]	-	-	-	-	0	0	58
Falls & Kopachena[S2]	-	-	-	-	1**	0	11
Horton et al.[S3]	-	-	-	-	0	1	602

Table S1, related to Figure 3. The frequencies of white-throated sparrows genotyped in this and other studies. Degradation of 2^m is caused by the rarity of homozygous ($2^m/2^m$) genotypes. The two $2^m/2^m$ females we identified were normal adult birds, as were the two females identified by Thorneycroft [S1] and Horton et al. [S3]. However, the one $2^m/2^m$ male chick we identified (*) was a runt from a WxW nest that was 45% below the average mass for a chick that age (>2 standard deviations below the mean), and 55% below the mass for its sibling (a tan male that was a day older), possibly suggesting that $2^m/2^m$ is lethal in males (see also Figure S3). Falls and Kopachena [S2] briefly report a $2^m/2^m$ male (**) but little information is given about its condition.

	WxW	WxT	TxW	TxT
Total # of Pairs	9	600	499	8
% of total pairs	0.8	53.8	44.7	0.7
% of disassortative pairs	-	54.6	45.4	-
% of assortative pairs	52.9			47.1
# of assortative pairs that are secondary	6			2
% of assortative that are secondary	67.0			25.0

Table S2, related to Figure 1. Pair type distribution for the Cranberry Lake population of white-throated sparrows for 1988 through 2014 (Male x Female). Polymorphism is maintained by disassortative mating. Only 1% of pairs are assortative, and of those, 47% are secondary, meaning that they form only after the initial pair member (who was of the opposite morph) disappeared.

Scaffold Name	Length	F_{st}	Order
NW_005081635.1	2,499,552	0.02	1
NW_005081812.1	685,102	0.02	1
NW_005081708.1	1,082,352	0.02	2
NW_005081569.1	6,428,133	0.31	2*
NW_005081577.1	5,965,185	0.31	3*
NW_005081742.1	823,114	0.33	4*
NW_005081832.1	313,837	0.31	5*
NW_005081548.1	11,897,188	0.33	6*
NW_005081699.1	1,154,867	0.31	7*
NW_005081620.1	3,174,558	0.33	8*
NW_005081574.1	5,686,916	0.33	9*
NW_005081589.1	4,450,299	0.33	10*
NW_005081596.1	4,337,631	0.33	11*
NW_005081611.1	3,579,899	0.33	12*
NW_005081596.1	4,337,631	0.33	13*
NW_005081591.1	4,472,293	0.33	14*
NW_005081642.1	2,137,341	0.33	15*
NW_005081561.1	7,563,313	0.33	16*
NW_005081632.1	2,519,554	0.33	17*
NW_005081596.1	4,337,631	0.33	18*
NW_005081561.1	7,563,313	0.33	19*
NW_005081582.1	4,953,235	0.33	20*
NW_005081569.1	6,428,133	0.31	21*
NW_005081654.1	1,929,533	0.30	22*
NW_005081553.1	10,164,019	0.26	23*

Table S3, related to Figure 2. Scaffolds and their order along chromosome 2 based on FISH mapping of BAC clones. Scaffold average F_{st} is provided for each. Scaffolds associated with BACs that mapped to the inverted region are highlighted with an asterisk.

	Pairtype (Male x Female)			
	WxW	WxT	TxW	TxT
Proportion of Male chicks ± SE (N)	0.32 ± 0.16 (6)	0.53 ± 0.02 (283)	0.48 ± 0.02 (241)	0.43 ± 0.16 (6)
Proportion of White chicks ± SE (N)	0.68 ± 0.14 (6)	0.49 ± 0.02 (283)	0.51 ± 0.02 (241)	0.26 ± 0.14 (6)
Proportion of EPP ± SE (N)	0.38 ± 0.18 (7)	0.28 ± 0.02 (199)	0.04 ± 0.02 (172)	0.41 ± 0.20 (6)

Table S4, related to Figure 3. Sex ratio, morph ratio and frequency of extra pair paternity (EPP) for the four different pair-types (N= number of pairs). White x White (WxW) assortative pairs produce female biased clutches and suffer a higher rate of EPPs. Tan x Tan pairs also suffer a higher rate of EPP relative to TxW pairs, which have the lowest rate of EPP. Note that white chicks found in TxT pairs are due to extra pair matings.

SUPPLEMETAL EXPERIMENTAL PROCEDURES

Field study: Field observations and samples were collected from a population of white-throated sparrows at the Cranberry Lake Biological Station in NY (44°07'N; 74°47'W) sampled between 1988 and 2014 (Master banding permit #22297 to E.M.T.). The field site supports ~100 pairs/season. Each pair was observed for a minimum of 80 hours over the entire season during which parental attendance at the nest, fledging, and predation were monitored. Blood samples were taken from nestling birds at post-hatch day 6, before they fledge the nest and while they are still completely dependent on parental provisioning. The sex of chicks was determined using standard protocols and primers [S5] and morph was determined using a PCR-based method, which amplifies the VIP gene and allows the identification of a morph-specific SNP [S2]. Paternity was determined using a combination of polymorphic microsatellite markers developed for other avian species [S6-S9]. To assign parentage we used the paternity analysis program CERVUS 3.0 [S10]. To test whether super white ($2^m/2^m$) birds are less common in the population that expected by chance we calculated their expected frequency based on the number of white male x white female (WxW) pairs and the frequency of extra-pair matings between white females and white males. Such extra pair matings should also produce 25% superwhite offspring. Based on our observations, WxW pairs comprise 0.8 % of the pairs in the population. Additionally, tan male x white (TxW) female pairs make up 44.7 % of the population but produce 4 % of offspring via extra pair mating with white males. Thus, based on sampling 1,989 birds from both within-pair and extra-pair matings, we would expect to see 12 superwhite chicks.

Fluorescent in situ hybridization: Candidate white-throated sparrow BAC clones (CHORI-264 [S11]) were identified using overgo probe hybridisation. BAC clones were grown and labeled following previously described protocols [S11,S12]. BAC DNA was labeled with SpectrumGreen®, SpectrumRed®, or SpectrumOrange® (Abbot Molecular, Inc. Abbot Park, Illinois) through nick translation. Homologous probes were hybridized to slides for 16 hours, heterologous probes and mixed heterologous/homologous probes were hybridized for 92 hours using probes of two different colours. Homologous probes were washed at 42 °C and all others were washed at 37 °C, following established stringency. Slides were

counterstained with DAPI III (Abbot Molecular Inc, Abbot Park, Illinois) and imaged using a multiphase microscope and fluorescent camera with CytoVision® software (Leica Biosystems, Germany).

Genome assembly: DNA was obtained from an adult tan morph male red blood cells (hematocrit) from one individual (karyotyped as *2*/*2*, *Z*/*Z*). Another chromosomal polymorphism also segregates within the species, but is not correlated with morph [S1, S13, S14]. The sequenced individual was also homozygous for this polymorphism (*3a*/*3a*). The genome sequencing plan followed the recommendations provided in the ALLPATHS-LG assembler [S15]. This model requires 45x sequence coverage each of fragments (overlapping paired reads ~180bp length) and 3kb paired end reads as well as 5x coverage of 8kb PE reads. Total assembled sequence coverage of Illumina instrument reads was 63.3X using a genome size estimate of 1.09 Gb. This first draft assembly scaffold gaps were closed where possible with mapping of the same reference assembly Illumina sequences and local gap assembly. Contaminating contigs, trimmed vector in the form of X's and ambiguous bases as N's in the sequence were removed. All contigs 200bp and smaller were removed.

Gene annotation: Prior to gene annotation the assembly was first masked with known repeats using RepeatMasker [S16] and WindowMasker [S17]. Annotation was done using the NCBI gene annotation pipeline which is fully described and publicly available (http://www.ncbi.nlm.nih.gov/genome/annotation_euk/process/). The essential modules of this pipeline are the alignment programs Splign ([S18]; cDNA) and ProSplign (protein) and an HMM-based gene prediction program Gnomon (http://www.ncbi.nlm.nih.gov/genome/guide/gnomon.shtml). Following manual checks of the gene annotation output we predict a total sparrow gene count of 15,121 with a mean length of 595 amino acids, similar to other avian genomes.

Genome resequencing: Twenty-four tan and 25 white morph males sampled above were chosen for resequencing. DNA was extracted using Qiagen DNeasy kits and samples were pooled in equimolar amounts for library generation. Library preparation for each pool was done using Illumina TruSeq Sample Prep Kit, and sequencing was done using TruSeq SBS kit version 3 and data was processed with Cassava 1.8.2. Sequencing was done on two lanes of a HiSeq2000, yielding 726,657,908 100bp paired end reads. Three additional white morph individuals were individually sequenced. These three individuals were previously collected in Chicago, IL, US [S19]. Library preps were done using the Kapa Biosystems Library Construction Kit and sequenced using their TruSeq Rapid SBS sequencing kit version 1. Samples were sequenced on a single lane of a HiSeq2500 and yielded over 65 million reads per sample and a total of 416,496,508 paired end (100bp) reads. We also sequenced whole genome of two outgroups, Harris' sparrow (*Zonotrichia querula*) and golden-crowned sparrow (*Zonotrichia atricapilla*) using specimens housed at the University of Alaska Museum. Library preparation for these species was done using the Kapa Biosystems Hyper Kit and TruSeq Rapid SBS sequencing kit version 2. Sequencing was then conducted on an Illumina Hi-Seq 2500 and yielded over 240 million paired-end (120 bp) reads per species.

Phylogenomic analysis: To place chromosomes *2* and 2^m into a phylogenetic context, we compared white-throated sparrow genomic data with mRNA-seq data from rufous-collared sparrow *(Zonotrichia capensis)*, white-crowned sparrow (*Zonotrichia leucophrys*) [S19], song sparrow (*Melospiza melodia*) [S19] and dark-eyed junco (*Junco hyemalis*) [S20] and whole genome sequencing of Harris' sparrow (*Zonotricia querula*) and golden-crowned sparrow (*Zonotricia atricapilla*). To do so, we mapped mRNA and gDNA reads from each outgroup species to the tan reference genome using *bwa mem* [S21]. gDNA reads from the tan pool of birds was mapped to the tan reference genome as described above; gDNA reads from the white pool of birds was mapped to the composite reference genome as described below (see '*Population genomic analysis'*). We then generated a super matrix of any informative sites and encoded sites that are polymorphic within species with their corresponding IUPAC ambiguity code. We partitioned this super matrix into two regions that either contain the $2/2^m$ inversion region or do not. The phylogeny of these species was inferred for each partitioned super matrix using RAxML [S22] with the GTRCAT mutation model. Bootstrap support values for each node were generated with 1000 bootstrap replicates. The topology produced above was compared against a tree where the tan and white morphs were

constrained as monophyletic. The Tan+White tree was built in RAxML [S22] under a CAT model with 100 random addition sequence (RAS) replicates, and support values were obtained via 100 bootstrap replicates. The likelihood of each tree given our data was obtained using FASTTREE 2 [S23], and following comparison methods were employed in CONSEL [S24]: approximately unbiased test (AU), two bootstrapping methods (NP & BP), Bayesian posterior probabilities (PP), Kishino-Hasegawa (KH), Shimodaira- Hasegawa (SH), weighted Kishino-Hasegawa (WSH), and weighted Shimodaira-Hasegawa (WSH). P-values were calculated for each metric and used to assess which topology best describes the data and whether the trees are significantly different

Population genomic analysis: Pooled reads were mapped to the assembled genome using *bwa mem* [S21] and genome-wide estimates of variant allele frequencies were estimated with *CRISP* [S25] or *mpileup* [S26]. Mapping and variant detection was performed with default base and mapping quality thresholds and at least two reads with alternative alleles were required to call a site as polymorphic. On average, read depth in both pooled samples was ~27.5X, and sites with low read depth (<5X) or high read depth (>80X) were discarded. Variants were annotated using *SnpEffect* [S27]. F_{ST} was estimated between tan and white pooled samples as,

$$F_{ST} = \frac{H_{tot} - H_{with}}{H_{tot}}$$

where H_{tot} is average heterozygosity between tan and white birds and H_{with} is average heterozygosity within tan and white birds. Sliding window estimates of F_{ST} were calculated in 100Kb windows with a 10Kb step size. Windows with less than 100 variants were excluded from analysis.

To estimate the fraction of variants within the inversion region that have F_{ST} ~0.33 (the expected value for variants that are fixed between tan and white birds), we modelled $logit(F_{ST})$ as a mixture of three normal distributions using the *mixtools* [S28] package in R [S29]. To avoid spurious parameter estimates, we removed variants with F_{ST} less than 0.0005. Parameters of the mixture distribution (mixture parameter, mean, and standard deviation) were estimated by randomly sampling 100 sets of 10,000 variants within the inversion and calculating the average estimate across these random sets of SNPs.

Pairwise genetic diversity (Θ_π) was estimated using *PoPoolation* [S30]. To estimate Θ_π on chromosome *2*, we utilized allele frequency estimates from the tan pool of birds. To estimate Θ_π on chromosome 2^m, we generate a pseudo-white reference genome by substituting any mutation at ~50% frequency within the $2/2^m$ region in the pool of white birds into the tan reference genome using GATK's FastaAlternativeReferenceMaker [S31]. We then performed competitive remapping by mapping reads from the white pool of birds to a composite reference genome containing both the reference tan and pseudo-reference white genomes. Competitive remapping of the white-pool successfully separated reads emanating from either chromosome *2* or 2^m (median read depth of *2* scaffolds = ~12X; median read depth of 2^m scaffolds = ~12X). As a negative control, we also performed competitive mapping of reads from the tan pool of birds to the composite genome (median read depth of *2* scaffolds = ~27X; median read depth of 2^m scaffolds = 0X). Sliding window estimates of Θ_π were calculated in sliding 1Mb windows with a 10Kb step size. Windows with less than 100 variants were excluded from analysis.

We estimated pair-wise linkage disequilibrium (r^2) between pairs of SNPs within the sequence reads using the 'direct estimate' method of LDx [S32]. We only considered sites with intersecting read depth greater than 5 and minor allele frequency at either locus > 15%. These thresholds have been found to produce accurate estimates of r^2 [S32]. We calculated average r^2 in 1bp distance bins separately for regions of the genome outside the inversion and inside the inversion for 2 and 2^m.

We calculated the Direction of Selection (DoS) statistic [S33] for each gene in the genome using either Harris' or golden-collared sparrow as outgroup. To calculate *dn* and *ds* for each outgroup, we mapped gDNA reads to either the tan reference genome (as above) or the white pseudo-reference genome. To

calculate *pn* and *ps* for either *2*, 2^m, or the remainder of the genome we only considered polymorphisms with minor allele frequency less than 15% with at least four reads supporting the polymorphism. The use of low frequency polymorphisms was necessary to ensure that polymorphisms contributing to *pn* and *ps* were not fixed differences between *2* and 2^m. To calculate DoS between *2* and 2^m we treated fixed differences between them as *pn* and *ps*. To estimate average DoS for various classes of genes (see Figure 2A) we calculated the weighted average DoS and weighted standard error [S33]. We calculated Fay and Wu's *H* in non-overlapping 50Kb windows genome-wide using either Harris' or golden-collared sparrow as outgroup species to polarize the allele frequency spectrum from the tan pool. Fay and Wu's *H* was estimated using *npstat* [S34].

Gene expression analysis. We examined patterns of gene expression in white and tan birds for genes inside and outside the inverted region. We utilized previously published *mRNA*-seq data from whole brain extracts from three white- and three tan-morph birds [S19]. We first mapped the *mRNA*-seq from each bird to the tan reference genome using *bwa mem*. Next, we constructed masked reference genome for each of the six birds based on polymorphisms identified in this first round of mRNA-seq mapping using *bedtools maskfasta* [S35] function. We then remapped *mRNA*-seq to these individually masked genomes using tophat2 [S36] and estimated differential expression using cuffdiff [S37].

Allele specific expression analysis. We examined patterns of allele specific expression (ASE) within and outside the inversion for three heterozygous ($2/2^m$) white birds. We utilized previously published *mRNA*-seq data from whole brain extracts [S19] and also resequenced genomic DNA from the same three birds. To avoid reference allele bias in ASE estimation, we first mapped *gDNA* of these three birds to the tan reference genome. We then masked (i.e., converted the reference allele to 'N') all sites in the reference genome that were found to be heterozygous in any of the three birds using *bedtools maskfasta* [S35] function. We mapped *mRNA*-seq data to the masked reference genome using *bwa mem* [S21] and estimated ASE as the fraction of 'tan' alleles (e.g., the reference allele in the unmasked genome) at exonic SNPs with minimum *mRNA*-seq read depth of 50 and maximum *gDNA*-seq read depth of 15. We further required that SNPs used for ASE estimation were heterozygous in all three birds. ASE estimates per SNP were then averaged across the three birds.

Confirmation of pooled genotyping. To confirm fixed difference between morphs identified in pooled genotypes, we resequenced the genomes of three individual white birds sampled from a different population than the pooled sample. As expected, 75% variants within the inversion are heterozygous in all three birds; note, given limited sequencing depth of individual birds (~10X) we expect that a fraction of truly polymorphic variants to appear homozygous thus explaining the discrepancy between the rate of fixed differences (75% versus 78.6%) observed in our individual and pooled based resequencing, respectively.

SUPPLEMENTAL REFERENCES

S1. Thorneycroft H.B. (1975). Cytogenetic study of white-throated sparrow, *Zonotrichia-albicollis* (Gmellin). Evolution. *29*, 611-621.

S2. Michopoulos V., Maney D.L., Morehouse C.B., and Thomas J.W. (2007). A genotyping assay to determine plumage morph in the white-throated Sparrow (*Zonotrichia albicollis*). Auk. *124*, 1330-1335.

S3. Horton, B. M., et al., Behavioral Characterization of a White-Throated Sparrow Homozygous for the ZAL2(m) Chromosomal Rearrangement. *Behav Genet* **43**, 60-70 (2013)

S4. Falls, J. B. Kopachena, J. G (2010) in *The birds of North America Online* (ed Poole, A.) (Cornell Laboratory of Ornithology, Ithaca).

S5. Griffiths R., Double M.C., Orr K., and Dawson R.J.G. (1998). A DNA test to sex most birds. Mol Ecol. *7*, 1071-1075.

S6. Poesel A., Gibbs H.L., and Nelson D.A. (2009). Twenty-one novel microsatellite DNA loci isolated from the Puget Sound white-crowned sparrow, Zonotrichia leucophrys pugetensis. Molecular Ecology Resources. *9*, 795-798.
S7. Dawson R.J.G., Gibbs H.L., Hobson K.A., and Yezerinac S.M. (1997). Isolation of microsatellite DNA markers from a passerine bird, Dendroica petechia (the yellow warbler), and their use in population studies. Heredity. *79*, 506-514.
S8. Petren K. (1998). Microsatellite primers from Geospiza fortis and cross-species amplification in Darwin's finches. Mol Ecol. *7*, 1782-1784.
S9. Jeffery K.J., Keller L.F., Arcese P., and Bruford M.W. (2001). The development of microsatellite loci in the song sparrow, Melospiza melodia (Aves) and genotyping errors associated with good quality DNA. Mol Ecol Notes. *1*, 11-13.
S10. Kalinowski S.T., Taper M.L., and Marshall T.C. (2007). Revising how the computer program CERVUS accommodates genotyping error increases success in paternity assignment. Mol Ecol. *16*, 1099-1106.
S11. Lear T.L., Lundquist J., Zent W.W., Fishback J., W.D., and Clark A. (2008). Three autosomal chromosome translocations associated with repeated early embryonic loss (REEL) in the domestic horse (Equus caballus). Cytogenetic and Genome Research. *120*, 117-122.
S12. Lear T.L., Brandon R., Piumi F., Terry R.R., Gu√©rin G., Thomas S., and Bailey E. (2001). Horse gene mapping report: Mapping of 31 horse genes in BACs by FISH. Chromosome Res. *9*, 261-262.
S13. Thorneycroft H.B. (1966). Chromosomal polymorphism in white-throated sparrow Zonotrichia albicollis (Gmelin). Science. *154*, 1571-157
S14. Romanov M., N, Dodgson J., B, Gonser R., A, and Tuttle E., M. (2011). Comparative BAC-based mapping in the white-throated sparrow, a novel behavioral genomics model, using interspecies overgo hybridization. BMC research notes. *4*, 211-211.
S15. Gnerre S., MacCallum I., Przybylski D., Ribeiro F.J., Burton J.N., Walker B.J., Sharpe T., Hall G., Shea T.P., Sykes S. et al. (2011). High-quality draft assemblies of mammalian genomes from massively parallel sequence data. Proc Natl Acad Sci USA. *108*, 1513-1518.
S16. Smit A.F.A., Hubley R., and Green P. (1996). RepeatMasker Open-3.0.
S17. Morgulis A., Gertz E.M., Schaeffer A.A., and Agarwala R. (2006). WindowMasker: Window-based masker for sequenced genomes. Bioinformatics. *22*, 134-141.
S18. Kapustin Y., Souvorov A., Tatusova T., and Lipman D. (2008). Splign: Algorithms for computing spliced alignments with identification of paralogs. Biology Direct. *3*, 20.
S19. Balakrishnan C.N., Mukai M., Gonser R.A., Wingfield J.C., London S.E., Tuttle E.M., and Clayton D.F. (2014). Brain transcriptome sequencing and assembly of three songbird model systems for the study of social behavior. PeerJ. *2*, e396.
S20. Stager M., Swanson D.L., and Cheviron Z.A. (2015). Regulatory mechanisms of metabolic flexibility in the dark-eyed junco (Junco hyemalis). J Exp Biol. *218*, 767-777.
S21. Li H. (2013). Aligning sequence reads, clone sequences and assembly contigs with BWA-MEM. arXiv:1303.3997
S22. Stamatakis A. (2014). RAxML version 8: A tool for phylogenetic analysis and post-analysis of large phylogenies. Bioinformatics. *30*, 1312-1313.
S23. Price, M. N., Dehal, P. S., and Arkin, A. P. (2010). FastTree 2–approximately maximum-likelihood trees for large alignments. PLoS ONE *5*, e9490.
S24. Shimodaira, H., and Hasegawa, M. CONSEL: for assessing the confidence of phylogenetic tree selection. Bioinformatics *17*, 1246–1247
S25. Bansal V. (2010). A statistical method for the detection of variants from next-generation resequencing of DNA pools. Bioinformatics. *26*, i318-i324.
S26. Li H., Handsaker B., Wysoker A., Fennell T., Ruan J., Homer N., Marth G., Abecasis G., and Durbin R. (2009). The Sequence Alignment/Map format and SAMtools. Bioinformatics. *25*, 2078-2079.
S27. Cingolani P., Platts A., Wang L., Coon M., Nguyen T., Wang L., Land S.J., Lu X., and Ruden D.M. (2012). A program for annotating and predicting the effects of single nucleotide polymorphisms, SnpEff: SNPs in the genome of Drosophila melanogaster strain w 1118; iso-2; iso-3. Fly. *6*, 80-92.

S28. Benaglia, T., Chauveau, D. R. Hunter, D. R. Young, D. S. Mixtools: An R package for analyzing finite mixture models. *Journal of Statistical Software* **32**, 1-29 (2009).
S29. R Core Development Team. R: A language and environment for statistical computing. (R Foundation for Statistical Computing, Vienna, 2014).
S30. Kofler R., Orozco-terWengel P., de M., N., Pandey R.V., Nolte V., Futschik A., Kosiol C., and Schlotterer C. (2011). Popoolation: A toolbox for population genetic analysis of next generation sequencing data from pooled individuals. PLoS ONE. *6*, e15925.
S31. McKenna A., Hanna M., Banks E., Sivachenko A., Cibulskis K., Kernytsky A., Garimella K., Altshuler D., Gabriel S., Daly M. et al. (2010). The genome analysis toolkit: A MapReduce framework for analyzing next-generation DNA sequencing data. Genome Res. *20*, 1297-1303.
S32. Feder A.F., Petrov D.A., and Bergland A.O. (2012). LDx: Estimation of Linkage Disequilibrium from High-Throughput Pooled Resequencing Data. PLoS ONE. 7.
S33. Stoletzki N., and Eyre-Walker A. (2011). Estimation of the neutrality index. Mol Biol Evol. 28, 63-70.
S34. Ferretti, L., Ramos-Onsins, S.E., Perez-Enciso, M. (2013). Population genomics from pool sequencing. Mol Ecol *22,* 5561-5576.
S35. Quinlan, A.R. and Hall, I.M. (2010). BEDTools: a flexible suite of utilities for comparing genomic features. Bioinformatics *26*, 841-842.
S36. Kim D., Pertea G., Trapnell C., Pimentel H., Kelley R., and Salzberg S.L. (2013). TopHat2: Accurate alignment of transcriptomes in the presence of insertions, deletions and gene fusions. Genome Biol. 14.
S37. Trapnell C., Roberts A., Goff L., Pertea G., Kim D., Kelley D.R., Pimentel H., Salzberg S.L., Rinn J.L., and Pachter L. (2012). Differential gene and transcript expression analysis of RNA-seq experiments with TopHat and Cufflinks. Nature Protocols. 7, 562-578.